ISSN 1027-5495. Functional Materials, 23, No.3 (2016), p. 387-393.
doi:http://dx.doi.org/10.15407/fm23.03.387 © 2016 — STC "Institute for Single Crystals"

Bi nanolines characterization by linear optical methods

V.V.Buchenko, A.A.Goloborodko

T.Shevchenko National University of Kyiv,
64/13 Volodymyrska Str., 01601 Kyiv, Ukraine

Received January 21, 2016

The present paper dedicated to experimental investigations of optical properties of Bi/Si(001) interfaces and Bi nanolines in a wide spectral range (1÷4 eV). The experimental study of optical absorption spectrum showed the widening of the optical band gap of Bi/Si(001) interfaces with increasing the bismuth coverage, whereas after nanolines formation the width of the optical band gap decreases. Features of the experimentally obtained reflectance anisotropy spectra and surface differential reflectance spectra concerned with changing of the silicon surface reconstruction from 2×1 to 1×1 with the increasing of the bismuth covering degree from 0.5 ML to 1 ML. The experimental study of reflectance anisotropy spectra and surface differential reflectance spectra of Bi nanolines shows that the bismuth atoms are still present on the surface of the substrate in small amount, but the optical properties of such structures are determined by Si dimers.

Keywords: bismuth, reflectance anisotropy spectroscopy, surface differential reflectance spectroscopy, adsorption, silicon.

Исследованы оптические свойства интерфейсов Bi/Si(001) и нанолиний висмута в широком спектральном диапазоне (1÷4 eV). Исследования спектра поглощения показали, что при увеличении степени покрытия висмутом происходит увеличение ширины оптической запрещенной зоны интерфейсов Bi/Si(001), тогда как после образования нанолиний ширина оптической запрещенной зоны уменьшается. Особенности экспериментально полученных спектров анизотропии отражения и поверхностного дифференциального отражения связаны с изменением реконструкции поверхности кремния от структуры 2×1 до 1×1, при увеличении степени покрытия висмутом от 0.5 МШ до 1 МШ. Экспериментальные исследования спектра анизотропного отражения и спектра поверхностного дифференциального отражения нанолиний висмута показывают, что атомы висмута до сих пор присутствуют на поверхности подложки в небольшом количестве, однако, оптические свойства такой структуры определяются димерами кремния.

Дослідження наноліній вісмуту лінійними оптичними методами. *В.В.Бученко, А.О.Голобородько.*

Досліджено оптичні властивості інтерфейсів Bi/Si(001) та нанолінії вісмуту в широкому спектральному діапазоні (1÷4 eV). Дослідження спектра поглинання показали, що при збільшенні ступеня покриття вісмутом відбувається збільшення ширини оптичної забороненої зони інтерфейсів Bi/Si(001), тоді як після утворення наноліній ширина оптичної забороненої зони зменшується. Особливості експериментально отриманих спектрів анізотропії відбивання та поверхневого диференціального відбивання пов'язані зі зміною реконструкції поверхні кремнію від структури 2×1 до 1×1, при збільшенні ступеня покриття вісмутом від 0.5 МШ до 1 МШ. Експериментальні дослідження спектра анізотропного відбивання та спектра поверхневого диференційного відбивання наноліній вісмуту показують, що атоми вісмуту досі присутні на поверхні підкладинки у невеликій кількості, однак, оптичні властивості такої структури визначаються димерами кремнію.

1. Introduction

One of the priorities of the modern condensed matter physics is a study of low dimensional systems. Growth and properties of nanoscale surface structures depend on the state of the substrate surface, including the surface tension [1–4]. Si(001) reconstructed surface has a structure that mostly consists of rows of dimers. These surface dimers consist of two silicon atoms, each of which formally has an attached dangling bond that contains a single electron. The dangling bonds of the Si surface dimers contribute to the high reactivity of Si(001) surface. It is well known that V-group elements (As, Sb, and Bi) are used to passivate Si(001) surface by saturating the Si dangling bonds [3, 5–7]. Adsorbed Bi atoms form addimers on the top of the silicon dimer rows and can break Si dimers [6, 8]. Bi/Si(001) is a suitable model system for testing optical techniques, such as reflectance anisotropy spectroscopy (RAS) and surface differential reflectance spectroscopy (SDRS), since it has been well characterized by many conventional surface techniques, including low energy electron diffraction [9, 10], STM [10, 11] and Auger electron spectroscopy [12, 13].

The RAS [14] and SDRS [15] are used recently for experimental studies of surface states of semiconductors and metals. Mentioned methods allow exploring the clean surfaces and interfaces, even under not high vacuum, and they can show the surface modification in a real time. One should note that RAS is a very sensitive technique of surface investigation and gives well-reproducible spectra [16]. It provides only anisotropy of the surface reflectance (RA), not the intrinsic optical response of the bulk Si, therefore the surface without any anisotropy does not have features in the RAS signal. Moreover, the change of the optical anisotropy due to adsorbing molecules contains some information about the mode of adsorption. In contrast, the SDRS consists in comparing the reflectance of a clean surface with the modified one and gives deeper information on the adsorption, because it provides the relative change of reflectance [17–20]. The both RAS and SDRS need theoretical background because interpretation of the results of such experiments is possible only with sufficiently strong correlation of the experimental and theoretical results.

The present paper deals with optical properties of Bi nanolines (NLs) on Si(001) surface. Comparison of optical spectra of the nanostructures with its morphology allows using the surface optical diagnostic methods during its industrial production.

2. Experimental

The experiments were carried out in an UHV preparation chamber with a basic pressure of $5\cdot 10^{-11}$Torr. Auger electron spectroscopy (AES) and scanning tunneling microscopy (STM) were available for additional sample characterization. 4°-Misoriented vicinal Si(100) samples were used in the present experiments. In this case single-domain surfaces are formed by narrow terraces, which are separated by double steps, where all Si dimers have the same orientation. This allows one to measure RA spectrum, which is induced by the specified orientation of Si dimers [21, 22]. After heating at 600°C during one night by direct-current heating, the Si samples were flashed at 1200°C for few seconds to remove the oxide layer [23]. Four flashes were necessary to ensure the total removal of the oxide layer and get a maximum of anisotropic signal [24].

Line arrays were created by depositing 0.5 (Bi/Si(001)–0.5 ML) and 1 (Bi/Si(001)–1 ML) monolayer (ML) of Bi on a clean silicon surface at a rate of about 0.07 nm/min in the desorption regime (Bi($N_{6,7}O_{4,5}O_{4,5}$ 101 eV) and Si($L_{2,3}VV$ 92 eV). Auger line intensities are used to measure the Bi deposition rate [12]). During deposition the substrate was raised to the maximum temperature of 450°C and after deposition the overlayers were annealed at this temperature for up to 15 min. Under these preparation conditions, perfectly straight, atomically perfect lines form on the Si(001) surface, each up to several hundred nanometers long [25].

All the optical measurements were performed at the room temperature by use of a self-made apparatus [26]. A halogen lamp in range of 450÷850 nm and a high pressure Xe lamp in range of 300÷550 nm are used, together with a monochromator and a Glan prism to select the polarisation of incident light. The incident light is reflected back from the sample surface, through the second Glan prism, into a photomultiplier.

Refraction (n) and absorption (κ) indexes and the interface thicknesses (d) are calculated with the help of ellipsometric parameters ψ and Δ ($\tan\psi e^{i\Delta} = r_y/r_x$, where r_x and

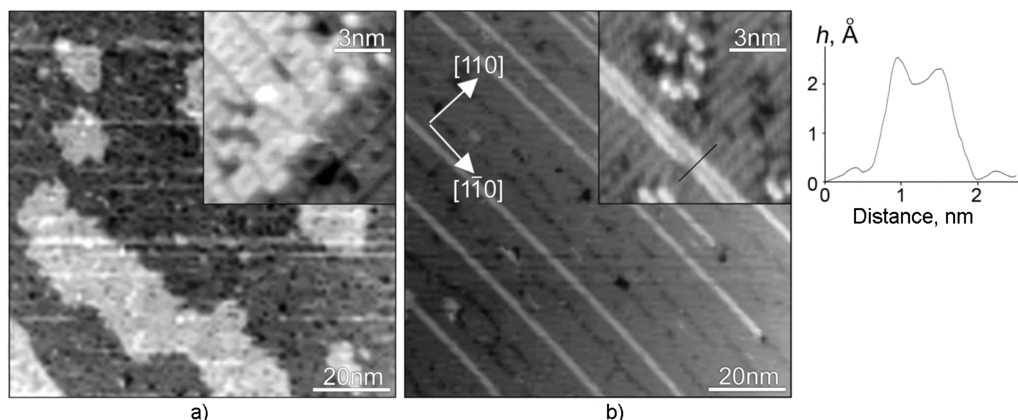

Fig. 1. STM image of 0.5 ML of bismuth (a) and Bi nanolines (b) on Si(001) surface. STM measurements were performed at the room temperature in constant current mode with negative sample bias (V_S) −1.5 V.

r_y are the complex incidence reflectances for two polarizations parallel to the principal axes for the (001) crystal face, along x and y directions, respectively, which are parallel and perpendicular to the Si–Si dimers, respectively), which are experimentally measured for the set of angles in a vicinity of the principal angle of incidence in the wide spectral range from 0.3 to 1.18 μm. Both n and κ values were calculated in the approximation of the thin Bi/Si(001) interfaces on the thick crystalline silicon substrate [27, 28].

The RA signal, defined as a real part of the difference between complex reflectances of amplitude, measured at normal incidence for two orthogonal polarizations of light:

$$I_{RAS} = 2\mathrm{Re}\left(\frac{r_x - r_y}{r_x + r_y}\right). \quad (1)$$

Ellipsometric parameters are measured in the experiments and the RA signal is defined as [29]:

$$I_{RAS} = 2\frac{1 - \tan^2\psi}{1 + \tan^2\psi + 2\tan\psi\cos\Delta}. \quad (2)$$

One should note the RA signal from the surface is relatively small and the effects of residual strain in the UHV-compatible window have to be taken into account to reduce it [30]. We defined "zero" position by using the oxidized Si(001) sample, with estimated error of about $2\cdot10^{-5}$.

The SDRS gives the reflectance difference between the clean surface and post-processed surface:

$$I_{SDRS} = \frac{R_{Bi/Si} - R_{Si}}{R_{Si}}, \quad (3)$$

where R_{Si} and $R_{Bi/Si}$ are the reflectivities (in intensity, i.e. the square of the reflectance: $R = |r|^2$ in the case of normal incidence) of the clean Si surface and of the Bi/Si(001) interfaces respectively. The surface differential reflectance (SDR) can be measured either with polarized or unpolarized light. The estimated error (defined by the series of measurements) is about $3\cdot10^{-5}$.

3. Results and discussion

Typical STM images of Bi/Si(001)–0.5 ML interface before and followed by annealing at 450°C are shown on Fig. 1. One can see that deposited Bi forms an island film on the Si(001) wide terrace (Fig. 1a), annealing at 450°C leads to Bi NLs forming (Fig. 1b). Length of the lines extends beyond the maximum field of view (100×100 nm^2). Recent high resolution STM image (inset image in Fig. 1b) shows some features (a double dot across the bismuth NLs), which appear on the STM image. One should note that these features tend to align diagonally with each other, even forming the local $c(4\times4)$ pattern in the places.

The NLs are formed by four dimers and have 15.8 Å wide. The bright dimerlike features making up the nanoline lie between the underlying Si dimers, in line with the Si dimer rows. As it was measured, the spacing between the nanoline features is 5.8 Å (Fig. 1). According to [31, 32] a simple nanoline model, with two adjacent Bi ad-di-

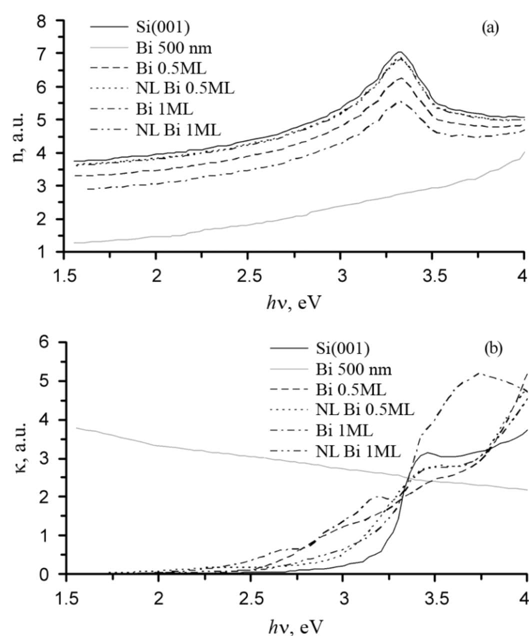

Fig. 2. Values of refraction (a) and absorption (b) indexes of Si(001) surface, 500 nm Bi coverage of Si(001) surface (Bi 500 nm), Bi/Si(001)–0.5 ML (Bi 0.5 ML) and Bi/Si(001)–1 ML (Bi 1 ML) interfaces, and corresponding Bi nanolines (NL Bi 0.5 ML, NL Bi 1 ML) as functions of incident photon energy.

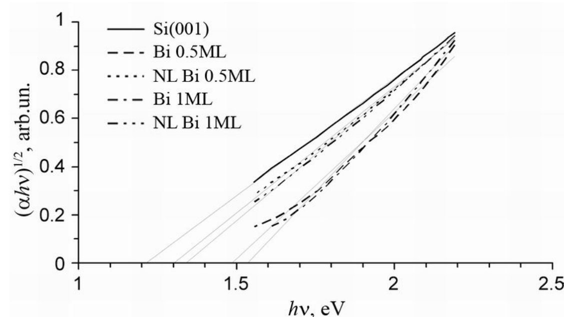

Fig. 3. Determination of the band gap of Si(001) surface, Bi/Si(001)–0.5 ML (Bi 0.5 ML) and Bi/Si(001)–1 ML (Bi 1 ML) interfaces, and corresponding Bi nanolines (NL Bi 0.5 ML, NL Bi 1 ML) as function of photon energy for indirect gap semiconductor $(\alpha h\nu)^{1/2}$.

mers sitting on top of the Si dimer row, reproduces most of the aspects of the detailed STM data.

The deposition of 1 ML of bismuth leads to perfect Bi film forming on the Si(001) surface. This film forms Bi nanolines with the higher concentration compared to the Bi/Si(001)–0.5 ML interface.

The values of refraction (n) and absorption (κ) indexes as functions of the incident photon energy are shown in Fig. 2. For comparison, Fig. 2 also presents the spectral dependences of n and κ for the crystalline silicon Si(001) and thick Bi film (thickness is of 500 nm) on the Si(001) substrate. Obtained optical constants are in a good agreement with the real and imaginary parts for silicon [33, 34] and bismuth [35, 36] given in the literature and determined using other characterization techniques. In our previous work [37], we have shown that simulation of spectral dependences of reflectivity can not be done using the simple optical model (air/smooth film/substrate). According to [38] the dependences of refraction and absorption indexes for thin layers, obtained at the same wavelength, aren't constant and can have different shapes first of all as a result of the differences in technological processes of the structure preparation. In fact, several parameters such Bi coverage rate, biaxial stresses and modification of the surface states must be taken into account in the calculation. Comparative analysis of n and κ spectral dependences shows that the feature of refraction index at energies $h\nu \approx 3.2 \div 3.4$ eV in Si(001) is reproduced well for Bi/Si(001) interfaces, with thicknesses of 0.5 ML and 1 ML, and Bi NLs, which are formed by these interfaces. One should note, that optical thicknesses of mentioned structures are 1.2 nm for Bi/Si(001) interfaces, 0.8 nm for Bi NLs and 487 nm for the thick Bi film. As one can see, the bismuth surface structures lead to modification of the surface states of Si (001) and may cause interface stress [39], which leads to appearance of differential optical conductivity. Significant feature of the absorption spectra is that κ values for Bi/Si (001) interfaces and Bi NLs are comparable to or even exceeds the corresponding value for Si (001) in the energy range of $h\nu > 2.5$ eV (the value of κ for bismuth less than the value of κ for Si(001) in the range of $h\nu > 3.4$ eV).

The band structure of the mentioned interfaces can also be revealed by analyzing the spectral dependence of $(\alpha h\nu)^{1/2}$, where $\alpha = 2\pi\kappa/\lambda$ is the absorption coefficient of the structure. Fig. 3 shows the spectral dependence of function $(\alpha h\nu)^{1/2}$ of vicinal Si(001) surface, Bi/Si(001) interfaces and Bi nanolines (formed by Bi/Si(001)–0.5 ML and Bi/Si(001)–1 ML) for determination of the band gap of the structures as indirect band

Table. General characteristics of the absorption edge in Bi/Si(001) systems

Sample	Band gap (E_g), eV
Si(001) [37]	1.13
Bi/Si(001)–0.5 ML [37]	1.48
NLs formed from Bi/Si(001)–0.5 ML (NL Bi 0.5 ML)	1.30
Bi/Si(001)–1 ML [37]	1.53
NLs formed from Bi/Si(001)–1 ML (NL Bi 1 ML)	1.34

gap semiconductors. The band gap (E_g) is determined by extrapolating the straight line portion of the spectrum to 0. The measurements reveal that the both Si surface and Bi/Si(001) interfaces are highly transparent in the IR range and have less intense adsorption in the range of 1.5–2.5 eV. Table exhibits the values of the band gap estimated from absorption spectra of Si(001) surface and Bi/Si(001) interfaces (E_g). The band gap for Si(001) at the room temperature corresponds to the fundamental Γ_{25}–X_1 transition and is 1.12 eV [40], which is in a good agreement with the value found in our study ($E_g \approx 1.13$ eV). One can see a blue shift of the absorption edge, i.e. the band gap widening is caused by Bi deposition. The increase of the band gap is caused by changes in the structure of the silicon surface, when the bismuth coverage increases from 0.5 ML to 1 ML. Herein, the Si(001) surface reconstructs from the structure 2×1 to 1×1, which is accompanied with the disappearance of σ (Si–Si) level, which corresponds to the bonds between the atoms of the surface Si dimers [37]. The Si dimers restoration and nanolines formation leads to decrease of the band gap.

Fig. 4 shows RAS spectra for vicinal Si(001), Bi/Si(001) interfaces (0.5 and 1 ML), and Bi nanolines formed by Bi/Si(001)–0.5 ML and Bi/Si(001)–1 ML. As shown by the experimental and theoretical studies, main contributions to the RA spectrum of vicinal Si (001) surface with energy below 3 eV originates from dangling bonds and steps. Important contribution is also due to bulk transitions modified in the vicinity of the surface. For the Si (001) surface spectrum a weak minimum at 1.45 eV is observed, this minimum is attributed to optical transitions between occupied and unoccupied surface bands corresponding to hy-

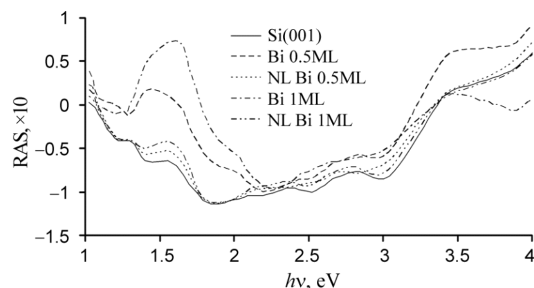

Fig. 4. Reflectance anisotropy spectra of vicinal Si(001) surface, Bi/Si(001)–0.5 ML (Bi 0.5 ML) and Bi/Si(001)–1 ML (Bi 1 ML) interfaces [37], and corresponding Bi nanolines (NL Bi 0.5 ML, NL Bi 1 ML).

bridization along the dimer rows of π and π^* states of the Si dimers [9, 41, 42]. On the other hand, according to theoretical calculations, the contribution of steps to the reflectance anisotropy spectrum appears as small peaks with positive sign in 1.5÷1.6 eV range and broad peaks with negative sign in 2.2÷3 eV range [41, 43].

All spectra (Fig. 4) have been obtained on vicinal Si(001) surface. It can be seen that Bi/Si(001) surface with the coverage of 0.5 and 1 ML exhibits interesting results: the RA spectrum contains peaks at 1.6 and 2.25 eV. When bismuth adsorbed on the Si surface is maintained at the room temperature, it results in a reordered surface, where the Si dimers are broken and Bi dimers appears. As a result, slight increase of intensity of the reflectance anisotropy spectra was observed around 1.5 eV at 0.5 ML Bi covering. In Fig. 4, the region about 1.6 eV shows dramatic changes after 1 ML deposition of Bi, the RAS spectrum becomes positive. However, theoretical calculations [37] show that there are no vertical transitions with energy 1.6 eV in Bi/Si(001)–1ML structure. The experimental study of the absorption spectra of Bi/Si(001)–1 ML surface shows no light absorption with energy 1.6 eV [37]. On the other hand, according to the principle of calculation of the reflectance anisotropy spectrum (2), subtraction of surface reflectivity for light with different polarization is normalized by total reflectivity of the surface. Thus, despite the small value of the total light absorption the reflectance anisotropy of the surface can be evaluated, and positive RAS data of Bi/Si(001)–1 ML (in the region around 1.6 eV) surface may be caused by the presence of S-type steps [44]. The RA spectra of NLs faintly differ from the RA spectra of

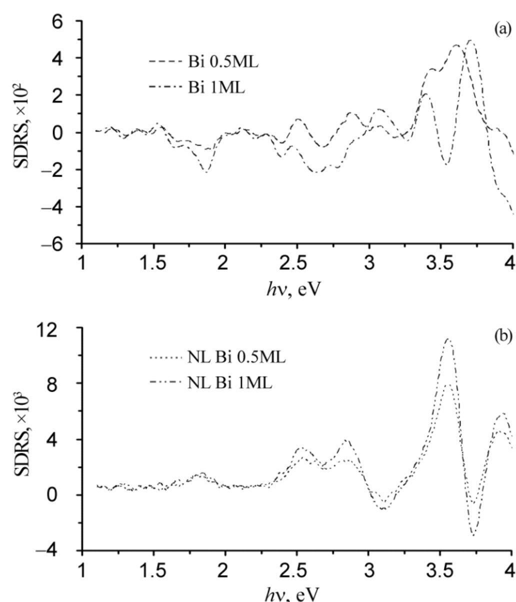

Fig. 5. Surface differential reflectance spectra of Bi/Si(001)–0.5 ML (Bi 0.5 ML) and Bi/Si(001)–1 ML (Bi 1 ML) interfaces [37] (a), and corresponding Bi nanolines (NL Bi 0.5 ML, NL Bi 1 ML) (b).

vicinal Si, because the Si features are dominating in the spectrum. As one can see (Fig. 1), Bi NLs covers a little of the Si surface, so the difference in reflectance is completely depend on Si, but some features around 1.6 eV indicates the presence of the Bi dimers.

According to [45], the SDRS provides more accurate determination of the spectral features due to exclusion of contribution from the substrate, and may unravel the bonding mode of different kinds of molecules on Si(001), which provides clear discrimination between the breaking of the surface Si dimers and their restoration upon the Bi nanolines formation [29]. Fig. 5 shows the surface differential reflectance spectra for the Bi/Si(001) interfaces with 0.5 and 1 ML of Bi covering and for Bi NLs formed by mentioned interfaces. Vicinal Si(001) is used as pure, preprocessed surface. According to [37] the sign of SDRS data for certain energy range is determined as relation between the values of light reflectivity of the clean substrate surface and the surface structure, created on this substrate. Herewith, negative values of the surface differential reflectance spectrum indicate, that the reflection coefficient of the clean substrate surface is greater than the reflection coefficient of the surface structure; positive values appear in the opposite case. The SDRS exhibits both transitions corresponding to the Si (001) surface and Bi atoms. Negative values of the SDR spectrum of the Bi/Si(001)–1 ML interface with energy below 3 eV corresponds to decrease of the light absorption after coating 1 ML of bismuth. One can see the SDRS minima near 1.8 eV (Fig. 5a), which correspond to the transition between the bonded (π) and antibonding (π^*) orbitals of the surface silicon dimers [46], for the Bi/Si(001) interfaces, and there is no minima at 1.8 eV for Bi nanolines (Fig. 5b). This feature appears after bismuth adsorption due to saturation of Si dandling bonds and disappears when surface of Si dimers restore upon Bi nanolines creation. Thus, the SDRS provides a possibility of distinguishing the spectral components, which correspond to the bismuth atoms adsorbed on the silicon surface.

4. Conclusions

We performed a complex study of the optical properties of Bi/Si(001) interfaces and Bi nanolines on Si(001) surface, and compared them with the corresponding parameters for crystalline Si(001).

The experimental results revealed the blue shift of absorption edge of Bi/Si(001) interfaces with increasing degree of bismuth coverage from 0.5 to 1 ML. We attributes this to the breaking of the Si dimer bonds and transformation of Si(001) surface structure from 2×1 to 1×1. Annealing at 450°C forms perfect Bi nanolines, restores Si dimer bonds and leads to decreasing the edge of absorption. The quantity or concentration of nanolines affects on the absorption edge.

RAS reveals the spectrum features around 1.6 eV and 2.25 eV. RAS signal in energy range near 1.6 eV increases with increasing the bismuth coverage and becomes positive for Bi/Si(001)–1 ML. The restoration of the Si dimers and Bi nanolines formation leads to decreasing the RAS signal near 1.6 eV.

Further work should be done, attempting to find the features of the RAS and SDRS signal formation. This allows to obtain information on the electronic structure and dynamics of the exited states in subsurface region.

References

1. D.J.Eaglesham, M.Cerullo, *Phys. Rev. Lett.*, **64**, 1943 (1990).

2. N.V.Nguyen, D.Chandler-Horowitz, P.M.Amirtharaj, J.G.Pellegrino, *Appl.Phys.Lett.*, **64**, 2688 (1994).
3. L.Fazi, C.Hogan, L.Persichetti et al., *Phys. Rev.B*, **88**, 195312 (2013).
4. J.Wang, Z.Huang, H.Duan et al., *Acta Mechanica Solida Sinica*, **24**, 52 (2011).
5. A.Hidehito, Y.Tatsuya, Y.Kenji et al., *Surf. Sci.*, **609**, 157 (2003).
6. T.V.Afanasieva, I.F.Koval, N.G.Nakhodkin, *Surf.Sci.*, **507**, 787 (2002)
7. W.Dorsch, S.Christiansen, M.Albrecht et al., *Surf.Sci.*, **331–333**, 896 (1995).
8. T.V.Afanasieva, *Ukr.J.Phys.*, **60**, 130 (2015).
9. M.Richter, J.C.Woicik, J.Nogami et al., *Phys. Rev.Lett.*, **65**, 3417 (1990).
10. J.Nogami, A.A.Baski, C.F.Quate, *Appl.Phys. Lett.*, **58**, 475 (1991).
11. D.H.Rich, F.M.Leibsle, A.Samsavar et al., *Phys.Rev.B*, **39**, 12758 (1989).
12. I.F.Koval, P.V.Melnik, N.G.Nakhodkin et al., *Surf.Sci.*, **331–333**, 585 (1995).
13. I.F.Koval, P.V.Melnik, N.G.Nakhodkin et al., *Surf.Sci.*, **384**, L844 (1997).
14. T.Bork, W.E.McMahon, J.M.Olson, T.Hannappel, *J.Cryst.Growth*, **298**, 54 (2007).
15. V.A.Funtikov, N.E.Antonova, *Glass Phys. Chem.*, **33**, 183 (2007).
16. A.Sassella, A.Borghesi, M.Campione et al., *Appl.Phys.Lett.*, **89**, 261905 (2006).
17. C.Noguez, C.Beitia, W.Preyss et al., *Phys. Rev.Lett*, **76**, 4923 (1996).
18. O.Pluchery, R.Coustel, N.Witkowski, Y.Borensztein, *J.Phys.Chem.B*, **110**, 22635 (2006).
19. Y.Borensztein, *Phys.Status Solidi (A)*, **202**, 1313 (2005).
20. M.Palummo, G.Onida, R.Del Sole, B.S.Mendoza, *Phys.Rev.B*, **60**, 2522 (1999).
21. T.Yasuda, M.Nishizawa, N.Kumagai et al., *Thin Solid Films*, **455–456**, 759 (2004).
22. L.Mantese, U.Rossow, D.E.Aspnes, *Appl.Surf. Sci.*, **107**, 35 (1996).
23. J.D.O'Mahony, J.F.McGilp, F.M.Leibsle et al., *Semicond.Sci.Technol.*, **8**, 495 (1993).
24. R.Ehlert, J.Kwon, M.C.Downer, *Phys.Status Solidi (C)*, **5**, 2551 (2008).
25. K.Miki, J.H.G.Owen, D.R.Bowler et al., *Surf. Sci.*, **421**, 397 (1999).
26. A.A Goloborodko, M.V.Epov, L.Y.Robur, T.V.Rodionova, *J.Nano-Electron.Phys.*, **6**, 020021 (2014).
27. T.V.Rodionova, A.S.Sutyagina, A.G.Gumenyuk, L.Y.Robur, *J. Nano- and Electron. Phys.*, **7**, 01033 (2015).
28. J.D.E.McIntyre, D.E.Aspnes, *Surf.Sci.*, **24**, 417 (1971).
29. V.V.Buchenko, A.A.Goloborodko, in: Proc. SPIE 9809, Twelfth Intern. Conf. Correlation Optics, Chernivtsi, Ukraine (2015), p.98090N-1.
30. Y.Borensztein, O.Pluchery, N.Witkowski, *Phys.Rev.Lett.* **95**, 1174021 (2005).
31. D.R.Bowler, J.H.G.Owen, *J.Phys.:Condens. Matter* **14**, 6761 (2002).
32. J.H.G.Owen, K.Miki, H.Koh, *Phys.Rev.Lett.*, **88**, 226104 (2002).
33. D.E.Aspnes, A.A.Studna, *Phys.Rev.Lett.*, **54**, 1956 (1985).
34. H.Touir, P.Roca i Cabarrocas, *Phys.Rev.B*, **65**, 155330 (2002).
35. A.P.Lenham, D.M.Treherne, R.J.Metcalfe, *J. Opt.Soc.Am.*, **55**, 1072 (1965).
36. P.Y.Wang, A.L.Jain, *Phys.Rev.B*, **2**, 2978 (1970).
37. V.V.Buchenko, A.A.Goloborodko, T.V.Afanasieva, *Materialwissenschaft und Werkstofftechnik*, **47**, 120 (2016).
38. S.A.Kovalenko, M.P.Lisitsa, *Semicond. Phys., Quant. Electron. & Optoelectron.*, **4**, 352 (2001).
39. L.V.Poperenko, A.A.Goloborod'ko, N.V.Epov, *J. Appl. Spectr.*, **82**, 744 (2015).
40. P.Y.Yu, M.Cardona, Fundamentals of Semiconductors: Physics and Materials Properties, Springer, Berlin, Heidelberg (1996).
41. W.G.Schmidt, S.Glutsch, P.H.Hahn, F.Bechstedt, *Phys.Rev.B*, **67**, 853071 (2003).
42. C.Hogan, R.Del Sole, G.Onida, *Phys.Rev.B*, **68**, 354051 (2003).
43. A.Hermann, W.G.Schmidt, F.Bechstedt, *Phys. Rev.B*, **71**, 1533111 (2005).
44. W.G.Schmidt, F.Bechstedt, *J.Bernholc, Phys. Rev.B*, **63**, 045322 (2001).
45. S.G.Jaloviar, Jia-Ling Lin, Feng Liu et al., *Phys.Rev.Lett.*, **82**, 791 (1999).
46. R.Shioda, J. van der Weide, *Phys.Rev.B*, **57**, R6823 (1998).